ELECTRONIC JOURNAL OF POLISH AGRICULTURAL UNIVERSITIES

2004
Volume 7
Issue 1
Series CIVIL ENGINEERING

MURAWSKI K. 2004. QUALITY DESCRIPTION OF FOLDING PHENOMENON OF THIN-WALLED CYLINDRICAL RODS MADE OF STEEL R 35 DURING LOSS OF STABILITY IN PLASTIC STATES **Electronic Journal of Polish Agricultural Universities**, Civil Engineering, Volume 7, Issue 1.
Available Online http://www.ejpau.media.pl

QUALITY DESCRIPTION OF FOLDING PHENOMENON OF THIN-WALLED CYLINDRICAL RODS MADE OF STEEL R 35 DURING LOSS OF STABILITY IN PLASTIC STATES

Krzysztof Murawski
Department of Machinery Design Fundamentals, Agricultural University of Poznan, Poland

ABSTRACT

A description of the folding phenomenon of thin-walled cylindrical axially compressed rods during loss of stability in plastic states is presented in the paper. The course of quasi-static load and rod deformation thanks to simultaneous camera filming with the divided screen method is analysed. Changes of crystal grains in a polished cross-section before and after the experiment made on a R35 steel rod (PN-73/H-72240) are presented.

Key words: stability, plastic state, thin-walled, rod.

INTRODUCTION

The folding phenomenon appearing during loss of stability of a thickset of thin-walled quasi-static axially compressed rods in plastic states was observed since the beginning of XIX century by: [1, 2, 3, 4, 5, 6, 7, 8, 9, 10, 11, 12, 13, 16, 17, 18, 19, 20, 21, 22, 23] and others.

In order to describe the folding phenomenon simultaneous filming with the divided screen method was used which allowed tracing the course of the quasi-static load and rod deformation. To understand what happens "inside" the tube the changes of crystal grains on a polished cross-section before and after the experiment are analysed.

A FOLDING PHENOMENON

The examined thin-walled cylindrical shapes, which during application of a loading through discs were fully plastifed in the critical cross section and, consequently, on cylinder surface there appeared *n* sinusoidal waves in the axial direction, and *m* sinusoidal waves occurred in the transverse plane. First waves came into being at the ends of tubes as a consequence of occurring there the greatest relative deformations along the generating line of the cylinder [14, 15]. In elastic states, relative deformations have a linear course from the greatest value, for the extreme transverse section, to the least value in the central section. It was possible that during the experiment two types of folds in the transverse plane (depending on the radius of stiffness of the tube) appeared: round folds (number of transverse sinusoidal half-waves $m = 2$) when the radius of stiffness was greater than the critical one, and polygonal folds ($m = 3, 4 \ldots$) - when the radius of stiffness was lesser than the critical [15]. We can meet then triangle, quadratic, pentagon, hexagon and others polygonal transverse folds. The number of sinusoidal transverse waves - *m* depends on the circumferential stiffness of the tube. The folding under quasi-static axial loading is a secondary effect of dynamic deformation (a vibration form) in consequence of an impulse. It appears in the longitudinal and circular direction during loss of stability in the most loaded or the most weakened (e.g. geometrical or material imperfection) point. From the experiments characteristic (wavy) graphs: force – shortness, on which suitable waves (or their parts) respond to particular folds were obtained.

The initial and some selected phases of this phenomenon are presented in Photos 1÷4 for a sample ϕ30x80x0.75 *mm*, (slenderness ratio λ =7.73), which was deforming in regular, triangle folds ($m = 3$). A graph from the whole test is presented in Fig.1. As shown on the graph, after reaching the limit of proportionality *H* the curve gets into the non-linear range in which grows digressively up to the critical point *kr*. After passing this point, there appears on the tube surface a plastic line around the tube circumference. It initiates formation of a longitudinal sinusoidal half-wave – the initial form of the first fold. The fold comes into being as a consequence of the development of the plastic line joint in the horizontal plane and of simultaneous approaching of one side of the half-wave to another one.

Fig. 1. Curve P(Δa) with marked stages of creation of triangle folds

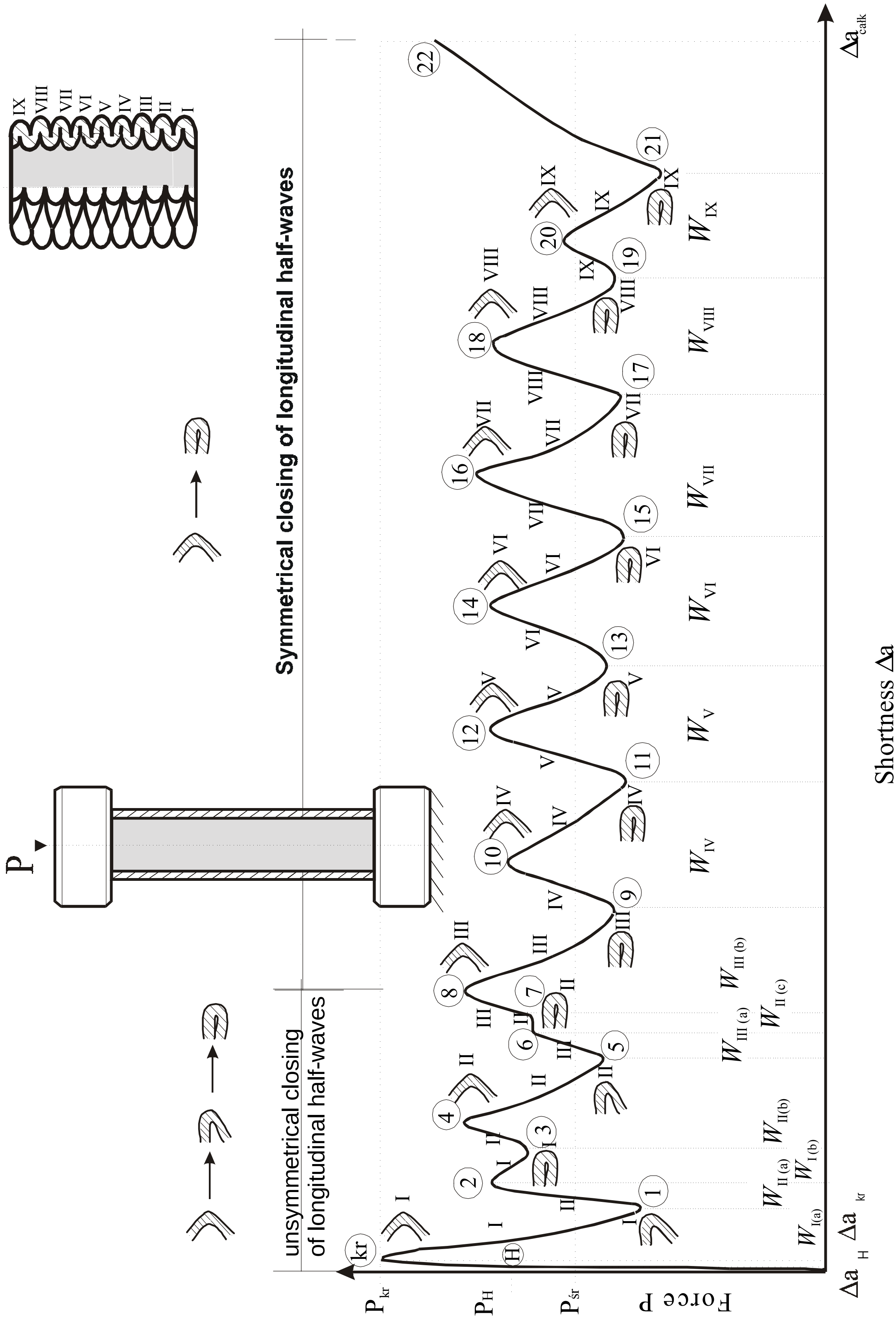

Photo 1. Initial phases of loading and deforming of the tube during creation of the triangle (*m*=3) plastic line joint around the tube circumference with unsymmetrical closing of longitudinal half-waves

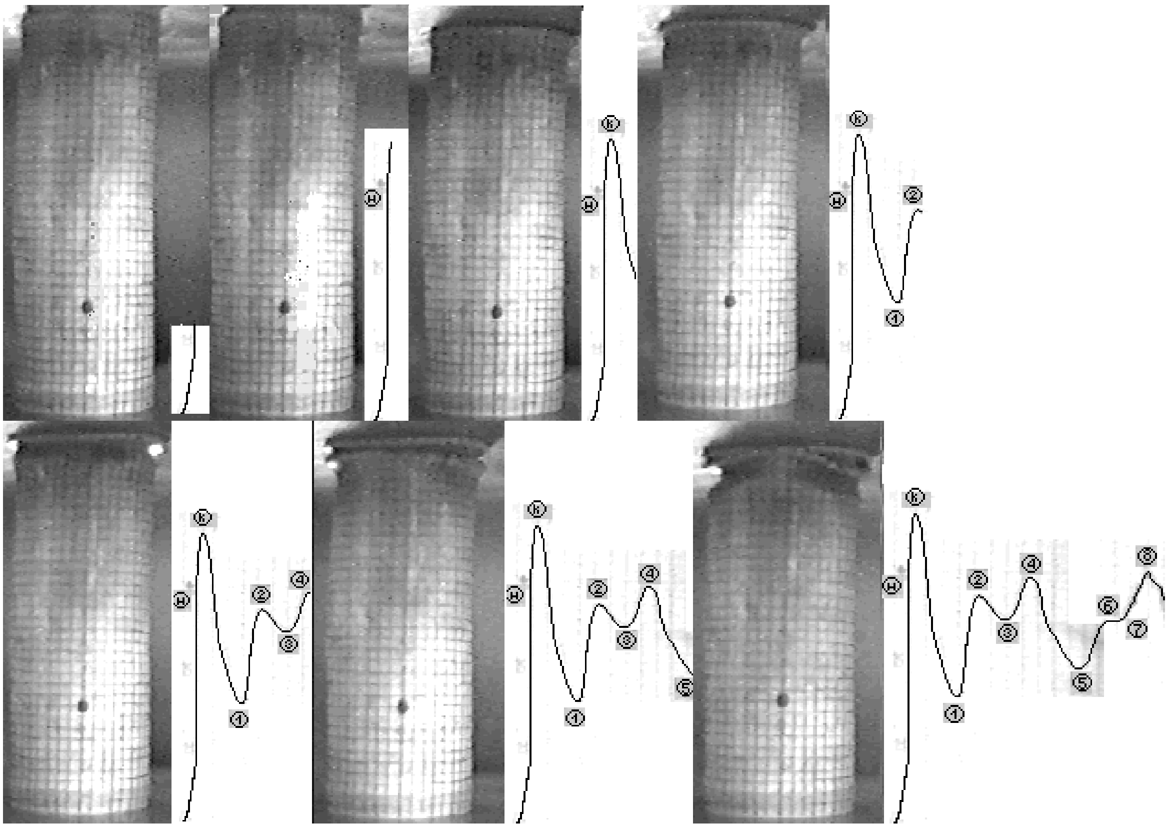

Photo 2. Phases of loading and deforming of the tube during creation of the triangle (*m*=3) plastic line joint around the tube circumference with symmetrical closing of longitudinal half-waves

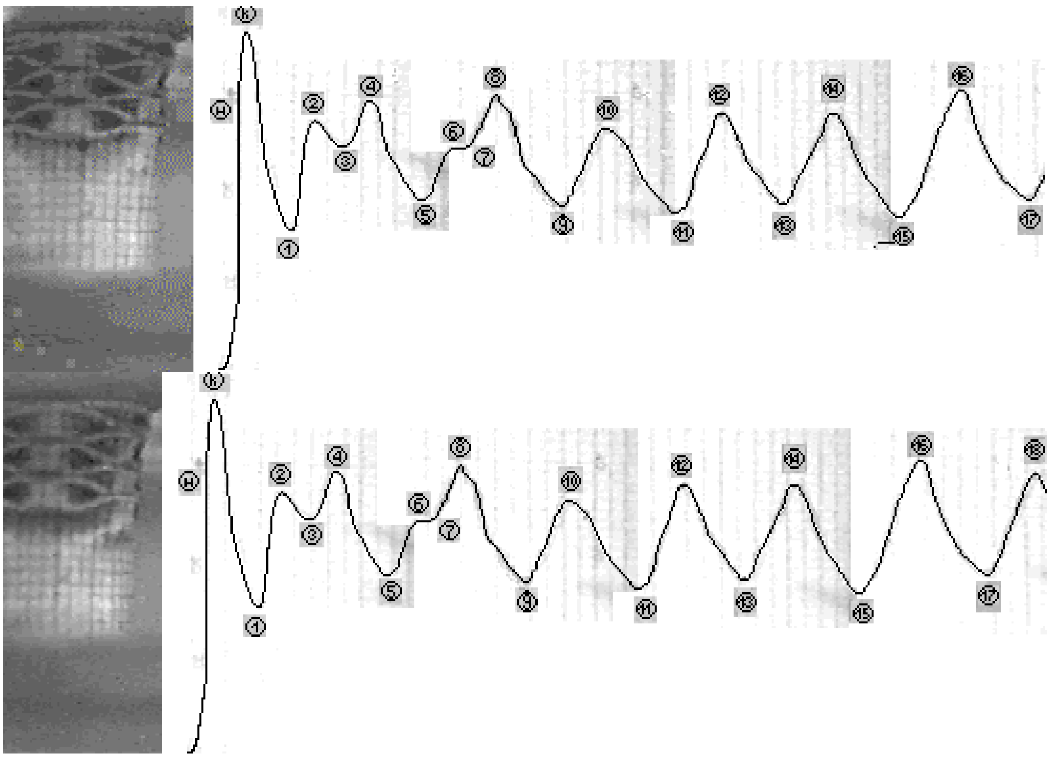

The external side approaches more quickly to horizontal surfaces than the internal side, causing asymmetric closing of the fold. There also occurs an additional plastic line joint around the tube circumference on the end of the internal side of the half-wave. During the approach of half-wave sides, the curve in the graph falls down to point 1. This fall, i.e. drop of the axial compressing force, is caused by increasing arm of this force with respect to the plastic joint. The growing up of the arm is an effect of translocation of the plastic lineal joint in the horizontal plane, so the current moment along this line is constant. In point 1, the first half-wave does not close yet. Between points 1 and 2 of the curve, a strengthening effect of the next layer closefitting to the first half-wave layer arises on the tube. In point 2, the resisting moment of the first half-wave becomes overcome again, and between points 2 and 3, the first fold is going to be finally closed. Between points 3 and 4, further strengthening of the next layer arises, and behind point 4 there appears a next circumferential plastic joint, which by analogy to the first one develops in stages between points 4, 5 and 6, 7. Between points 5 and 6, there arises further strengthening of the next tube layer, yet of the third half-wave. During these repeating processes, unsymmetrical closing of longitudinal half-waves up to point 8 takes place. Between points 8 and 9 there goes already full, one-stage development of the longitudinal half-wave with symmetrical closing. Between points 9 and 10, one-stage strengthening of the tube layer for the next half-wave is observed. During these repeating processes symmetrical closing of longitudinal half-waves up to point 22 take place.

In Fig. 1 stages of the formation of each fold and separated areas under the curve corresponding to the work done during emergence of each fold is schematically presented. Greater work regulared to realize the first stage of creation of the first fold as well as high value of the critical force, ensues from the activation phenomenon.

The course of the quasi-static load and rod deformation recorded by camera with the divided screen application is presented in the film.

CHANGES OF CRYSTAL GRAINS

To recognize the changes of crystal grains in the plastic line joint, longitudinal polished cross-sections with dimensions 1x10 and 3.2x10 mm^2 (Fig.2) of not deformed and deformed tubes made of steel R35 with a diameter of ϕ28x1 and the slenderness ratio $\lambda = 5$ were made.

Created polished microsections were prepared for observations under the microscope “EPITYP 2” producing enlargement by 50x and 100x and then were photographed (Photo 3). After that, the polished microsections were subject to quantity analysis with the “EPIQUWANT” device. The number of grains inside squares of 0.4x0.4 mm^2 along the base lines in the radial and circumferential directionswas later computed.

Fig. 2. The longitudinal cross-section subject to polishing (a) and crystal grain geometry after deformation (b)

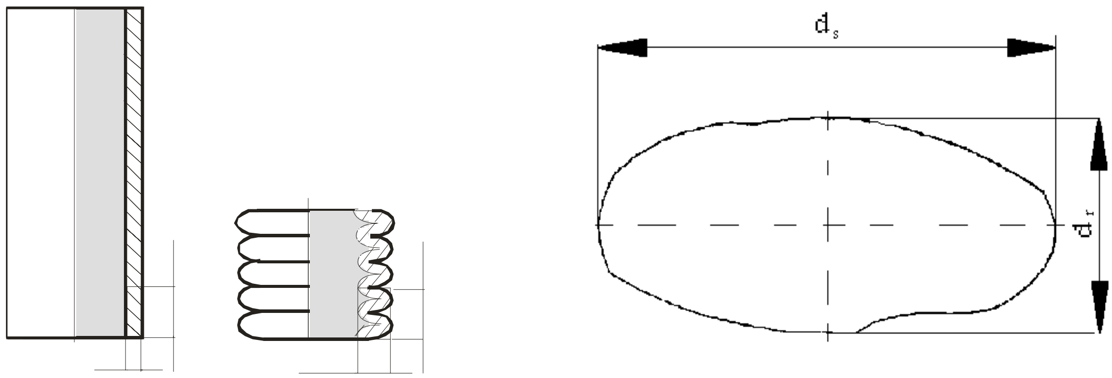

a) b)

Photo 3. The microstructure of steel R35 polished and micro-etched microsections: a) from a undeformed, b) from a deformed tube. The enlargement: 50x and 100x

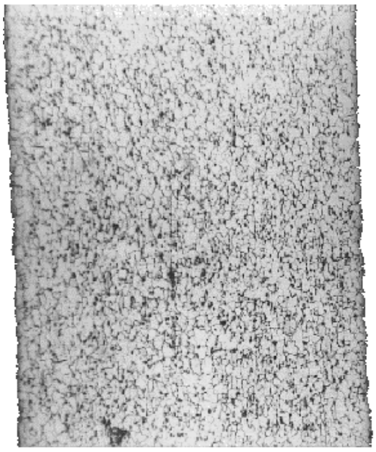

a)

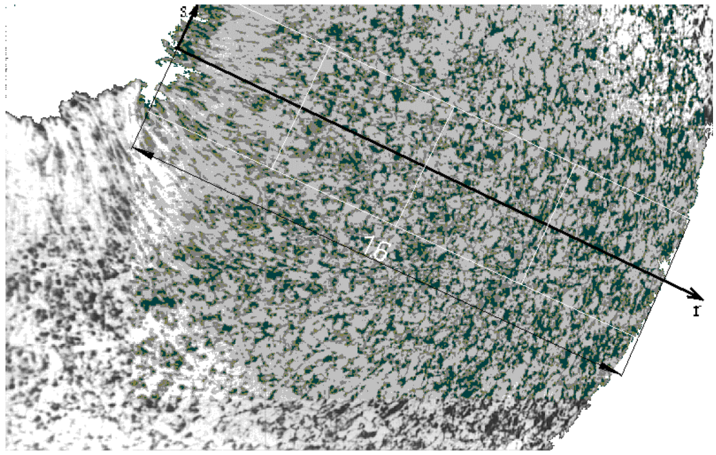

b)

Table 1. Results of quantity metallographic analysis of polished microstructured longitudinal cross-section of the fold

r *mm*	L_s *mm*	L_r *mm*	N_s	N_r	S_s μm^{-1}	S_r μm^{-1}	d_s μm	d_r μm	*k*
0.2	4720	6800	273	194	57.83	28.59	17.289	35.050	2.03
0.6	3800	2596	195	98	51.32	37.75	19.487	26.480	1.36
1.0	6000	6400	235	277	39.17	43.28	25.530	23.100	0.91
1.4	5912	6285	131	330	22.16	52.51	45.129	19.040	0.42

Fig.3. Course of the values of the axial size of deformed grains in the radial direction - d_r and in the circumferential direction - d_s along the radial coordinate - r

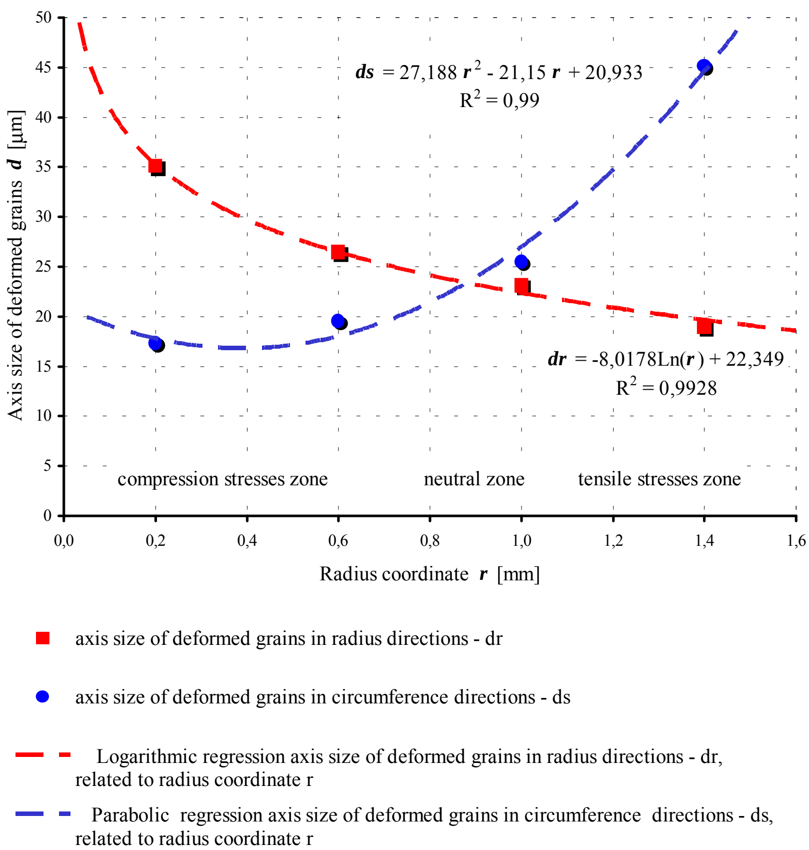

The total length of the base lines inside the squares in the radial direction is denoted by L_r, while in the circumferential direction – by L_s. The number of grains in the radial direction is denoted by N_r, in the circumferential one by N_s. The middle points of squares were 0.2, 0.6, 1.0, and 1.4 *mm* from the inside contour line of the fold (Photo 4). According to the analysis, the determined number of grains per millimetre in the radial direction was S_r, in the circumferential direction - S_s. The axial size of deformed grains in the radial direction was d_r, in circumferential one - d_s (Fig.3). Then the deformation ratio k for the tensioned and compressed sides according to the formula:

$$k = d_r / d_s. \quad (1)$$

was calculated.
The results are presented in Tab.1.

Fig. 4. A graph of the deformation ratio k along the radial coordinate r (Photo 3 and the upper outline in Photo 4)

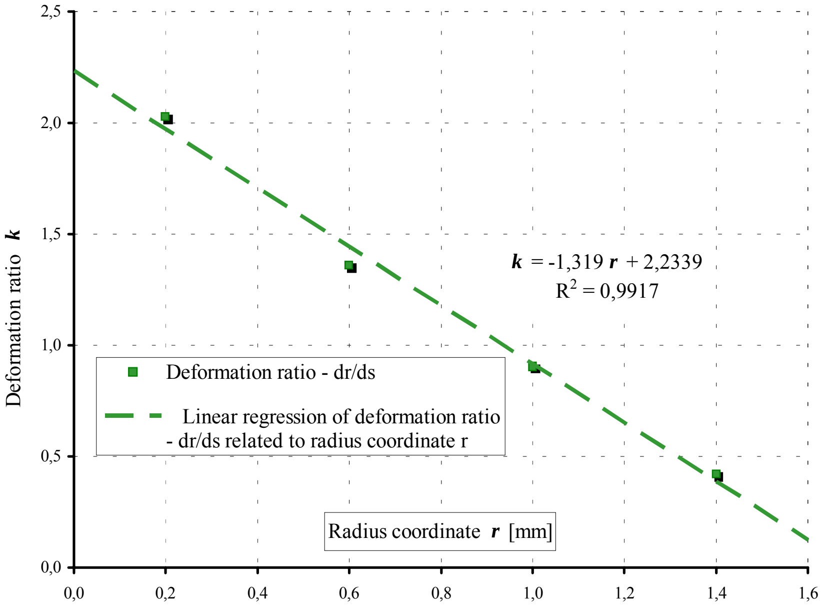

Photo 4. The microstructure of steel R35 polished and micro-etched microsections. The enlargement: 100x. Pearlite (light area) + ferrite (dark area)

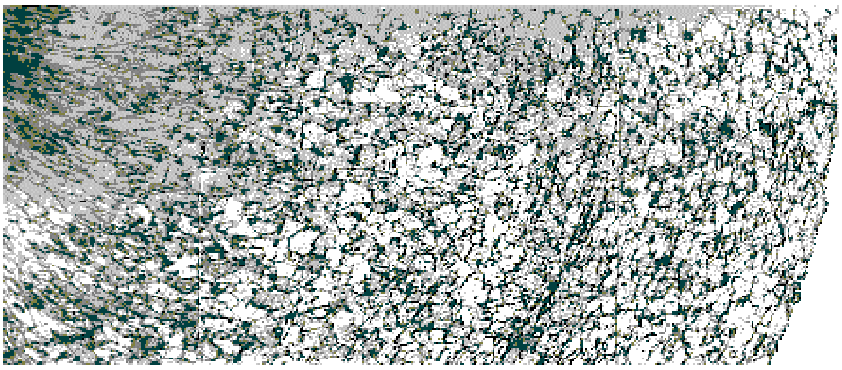

An approximated course of the deformation ratio k along the radial coordinate r of the fold is presented in Fig.4 above the deformed microstructure. This course shows changes of the deformation ratio k along the neutral layer of bending, and also shows where the neutral layer is. We can see there very clearly the compression and tensile stress areas. We can distinguish three zones:

1. tensile stresses zone – external (elongations of grains in the circumferential direction),
2. neutral zone – median (no elongations of grains – like in a undeformed microstructure),
3. compression stresses zone - (elongations of grains in the radial direction).

REFERENCES

1. Abramowicz W., Wierzbicki T., Bhat S. U., Brodkin D.,1992. Alexander Revisited - A Two Folding Elements Model of Progressive Crushing of Tubes. *Int. J. Solids and Struct*. 29: 1, 3269-3288.
2. Alexander J. M.,1960, An approximate analysis of the collapse of thin cylindrical shells under axial loading. *Quart. J. Mech. Appl. Math*. XIII: 1.
3. Donnel L. H., 1934. A New Theory for the Buckling of Thin Cylinders under Axial Compression and Bending. Trans. Amer. Soc. Mech. Engr. 56, 795-806.
4. Föppl L.,1926. Achsensymetrisches Auskniken zylindrischer Schalen. Sitzungsber. Bayer. Akad. Wiss., math.-naturwiss. Abt., 27-40.
5. Geckeler J. W.,1928. Plastisches Knicken der Wandung von Hohlzylindern und einige andere Faltungserscheinungen an Schalen und Blechen. Z. angew. Math. Mech. 8, 341-52.
6. Johnson W., Soden P. D., Al-Hassani S. T. S.,1977. Inextensional Collaps of Thin-Walled Tubes Under Axial Compression. *Journal of Strain Analysis* 12: 4.
7. Kaufmann W., 1935. Plastisches Knicken dünnwandiger Hohlzylinder infolge axialer Belastung. Ing.-Arch. 6, 334-37.
8. Kirste L., 1954. Abwickelbare Verformung dünnwandinger Kreiszylinder. Oster. Ingr.-Arch., 8 No 2-3.
9. Lorenz R., 1911. Achsensymetrische Verzerrungen in dünnwandingen Hohlzylindern. Z. Ver. deutsch. Ing. 52, 1706-13.
10. Łukasiewicz S., 1972. On the post-buckling behaviour of the cylindrical shell. Report No 468. Laboratory of Engineering Mechanics. Delft.
11. Mallock A., 1908. Note on the instability of tubes subjected to end pressure and on the folds in a flexible material. Proc. Roy. Soc. A, 81.
12. Mamalis A. G., Manolakos D. E., Viegelahn G., Johnson W.,1988. The Modelling of Progressive Extensible Plastic Collaps of Thin-Wall Shells. *Int. J. Mech. Sci*. 30:3/4, 249-261.
13. Mises R., 1914. Der kritische Aussendruckzylindrischer Rohre. Z. Ver. deutsch. Ing. 58,750-55.
14. Murawski K.,1992. Stability of thin shell columns in plastic states. *14 Międzynarodowe Sympozjum Naukowe Studentów i Młodych Pracowników Nauki*, Zielona Góra.
15. Murawski K., 2002. The Engesser-Shanley Modified Theory of Stability of Thin-Walled Cylindrical Rods with Example of Use for Steel St35. Acta Scientiarum Polonorum Architectura-Budownictwo 1-2 (1-2), 85-95.
16. Pugsley A. and Macaulay M.,1960. The Large-Scale Crumpling of Thin Cylindrical Columns, *Quart. J. Mech. Appl. Math*. XIII:1.
17. Southwell R. V., 1915. On the Collapse of Tubes by External Pressure. Philos. Mag. 25, 687-98, 1913, 26, 502-11,1913, 29, 67-77, 1915.
18. Sturm R. G., 1941. A Study of the Collapsing Pressure of Thin-Walled Cylinders. Bull. Illinois Engrg. Exper. Stat. No 239.
19. Szyszkowski W., 1975. Geometrical Analysis of Post-Buckling Behaviour of Thin Cylindrical and Conical Shells under Axial Compression. Archive of Machinery Structures, XXII, No 1, 3-25.
20. Tennyson R. C., 1964. Buckling of circular cylindrical shells in axial compression. AIAA Journal.
21. Thielman W. E. and Esslinger M. E., 1966. On the post-buckling behaviour of thin walled axially compressed circular cylinders of finite length. Dtsch. Forschungsangstalt Luft-u. Raumfahrt, Inst. für Flugzeugbau, Braunschweig 1966.
22. Wierzbicki T. and Bhat S. U., 1986. A Moving Solution for Axisymmetric Crushing of Tubes. Int. J. Mech. Sci., Vol. 28, No 3, 135-151.
23. Yoshimura Y., 1951. On the mechanism of buckling of circular cylindrical shell under axial compression. Repts. Inst. Sci. and Techno. Univ. Tokio, 5 No 5.

Krzysztof Murawski
Department of Machinery Design Fundamentals
Agricultural University of Poznan
Wojska Polskiego 38/42, 60-627 Poznan, Poland
e-mail: kmurawski@woodcock.au.poznan.pl
tel. 061 8487491, fax. 061 8487481
